Molecular Biology of the Cell
Vol. 16, 2058–2067, April 2005

SNX9 Regulates Dynamin Assembly and Is Required for Efficient Clathrin-mediated Endocytosis[V]

Fabienne Soulet, Defne Yarar, Marilyn Leonard, and Sandra L. Schmid

Department of Cell Biology, The Scripps Research Institute, La Jolla, CA 92037

Submitted November 19, 2004; Revised January 7, 2005; Accepted January 29, 2005
Monitoring Editor: Suzanne Pfeffer

Dynamin, a central player in clathrin-mediated endocytosis, interacts with several functionally diverse SH3 domain-containing proteins. However, the role of these interactions with regard to dynamin function is poorly defined. We have investigated a recently identified protein partner of dynamin, SNX9, sorting nexin 9. SNX9 binds directly to both dynamin-1 and dynamin-2. Moreover by stimulating dynamin assembly, SNX9 stimulates dynamin's basal GTPase activity and potentiates assembly-stimulated GTPase activity on liposomes. In fixed cells, we observe that SNX9 partially localizes to clathrin-coated pits. Using total internal reflection fluorescence microscopy in living cells, we detect a transient burst of EGFP-SNX9 recruitment to clathrin-coated pits that occurs during the late stages of vesicle formation and coincides spatially and temporally with a burst of dynamin-mRFP fluorescence. Transferrin internalization is inhibited in HeLa cells after siRNA-mediated knockdown of SNX9. Thus, our results establish that SNX9 is required for efficient clathrin-mediated endocytosis and suggest that it functions to regulate dynamin activity.

INTRODUCTION

The GTPase dynamin plays a critical role in clathrin-mediated endocytosis (CME; Hinshaw, 2000). Dynamin self-assembles into a collar-like structure around the necks of deeply invaginated clathrin-coated pits (CCPs) where it is believed to directly mediate membrane fission and vesicle release. Dynamin is also associated with newly formed coated pits (Damke *et al.*, 1994; Evergren *et al.*, 2004) where it may function to regulate early stages of coated pit maturation (Sever *et al.*, 2000a; Song and Schmid, 2003; Song *et al.*, 2004).

Although only one isoform of dynamin exists in *Drosophila* and in *Caenorhabditis elegans*, mammals express at least three isoforms, which are ~70% identical to each other. Dynamin-1, the first identified protein in the dynamin family, is expressed exclusively in neuronal cells where it functions in synaptic vesicle recycling (Shpetner and Vallee, 1989; Nakata *et al.*, 1991; Sontag *et al.*, 1994). Dynamin-2 is ubiquitously expressed (Cook *et al.*, 1994; Sontag *et al.*, 1994) and localizes to endocytic CCPs where it functions, like dynamin-1, in endocytosis (Damke *et al.*, 1994; Altschuler *et al.*, 1998). However, dynamin-2 may also be involved in vesicle formation at the Golgi (Cao *et al.*, 2000; Kreitzer *et al.*, 2000), in regulating actin dynamics (Schafer, 2004), in cell signaling (Kranenburg *et al.*, 1999; Fish *et al.*, 2000), and has recently been localized to the centriole (Thompson *et al.*, 2004). Dynamin-3, which is most highly expressed in testis but also detectable in neurons (Gray *et al.*, 2003) and in lung (Nakata *et al.*, 1993), has been less well studied.

Dynamins are atypical GTPases, distinguished by their large size, low affinity for GTP, and high intrinsic rates of GTP hydrolysis (Sever *et al.*, 2000b; Song and Schmid, 2003). Moreover, dynamin can self-assemble in solution (Hinshaw and Schmid, 1995) or on liposome templates into rings and spiral-like structures (Stowell *et al.*, 1999). Self-assembly in vitro stimulates dynamin's GTPase up to 50-fold (Sever *et al.*, 1999; Stowell *et al.*, 1999).

The function(s) of dynamin in CME may in part be dependent on its interactions with numerous SH3 domain-containing proteins, referred to as endocytic accessory factors. These proteins, which interact with dynamin through its C-terminal pro/arg-rich domain (PRD), fall into several functionally distinct classes. They include actin-binding proteins, e.g., cortactin and mAbp1 (McNiven *et al.*, 2000; Kessels *et al.*, 2001); scaffolding molecules, e.g., intersectin, syndapin, grb2, and nck, which link dynamin to N-WASP and other proteins (Gout *et al.*, 1993; Roos and Kelly, 1998; Peter *et al.*, 2004; Schmitz *et al.*, 2004); and membrane-active molecules, e.g., endophilin and amphiphysin, that can sense and/or generate membrane curvature (Schmidt *et al.*, 1999; Farsad *et al.*, 2001; Peter *et al.*, 2004). In the case of actin dynamics, there is growing evidence that dynamin can regulate the activity of some of these accessory proteins (Schafer *et al.*, 2002). There is also evidence, in turn, that some of these accessory proteins can regulate dynamin's GTPase activity (Wigge *et al.*, 1997). However, the functional interplay between dynamin and its accessory factors, and the role they play in CME, or in other dynamin related activities, remain poorly understood.

SNX9 is an SH3 domain-containing protein that interacts with both AP2 and clathrin (Lundmark and Carlsson, 2002, 2003) and was recently shown to interact with dynamin (Lundmark and Carlsson, 2003). SNX9 belongs to the sorting

This article was published online ahead of print in *MBC in Press* (http://www.molbiolcell.org/cgi/doi/10.1091/mbc.E04–11–1016) on February 9, 2005.

[V] The online version of this article contains supplemental material at *MBC Online* (http://www.molbiolcell.org).

Address correspondence to: Sandra L. Schmid (slschmid@scripps.edu).

Abbreviations used: CME, clathrin-mediated endocytosis; CCP, clathrin-coated pit; CCV, clathrin-coated vesicle; TfnR, transferrin receptor; amph1, amphyphisin-1; $PI4,5P_2$, phosphatidyl inositol-4,5-bisphosphate; TIR-FM, total internal reflection fluorescence microscopy; WF-EF, wide-field, epifluorescence; EGFP, enhanced green fluorescent protein; mRFP, monomeric red fluorescent protein.

nexin (SNX) family of structurally and functionally diverse proteins, defined by the presence of a phox (*ph*agocyte *ox*idase) homology domain (PX) that encodes a proline-rich sequence and an upstream phospholipid-binding domain (Cheever *et al.*, 2001). So far, 25 human SNXs have been identified and recent studies have uncovered a role for several of these proteins in membrane trafficking (Worby and Dixon, 2002). SNX9, also called SH3PX1, has in addition to its PX domain, an SH3 domain, and a BAR (Bin/amphiphysin/Rvs) domain, thought to be involved in lipid binding, curvature sensing, and dimerization (Habermann, 2004; Peter *et al.*, 2004). Like other sorting nexins, SNX9 interacts with several transmembrane proteins including Dscam in *Drosophila*, the insulin receptor and two metalloprotease disintegrins, MDC5 and MDC15 (Howard *et al.*, 1999; Worby *et al.*, 2001; MaCaulay *et al.*, 2003). SNX9 has also been linked to the actin cytoskeleton through its interaction in *Drosophila* with the orthologue of WASP (Worby *et al.*, 2001). Finally, several studies have suggested a potential role for SNX9 in clathrin-mediated endocytosis based on its interaction with components of the CME machinery (Lin *et al.*, 2002; Lundmark and Carlsson, 2002, 2003; Miele *et al.*, 2004).

Here we show that SNX9 directly regulates dynamin self-assembly activity in vitro and that in vivo SNX9 is required for efficient clathrin-mediated endocytosis and is transiently recruited to CCPs, coincident with dynamin, at a late stage in vesicle formation.

MATERIALS AND METHODS

Cells and Cell Culture

tTA-HeLa cells that express the chimeric tetracycline (tet)-regulatable transcription factor were obtained from Clontech (Palo Alto, CA) and cultured in DMEM containing 10% fetal calf serum (FCS) and 0.1 mg/mg G418, as previously described (Damke *et al.*, 1994) In these cells, the presence of tetracycline suppresses expression from a tet-responsive promoter element.

Constructs and Generation of Recombinant Adenoviruses

The cDNA for SNX9 was subcloned from pcDNA3-HA-SNX9 (Lin *et al.*, 2002) into pGEX.KG with *Bam*HI/*Eco*RI digestion. SNX9ΔSH3 cDNA was generated by PCR followed by subcloning into the *Bam*HI/*Eco*RI sites of pGEX.KG and for HA-SNX9ΔSH3 into *Hin*dIII/*Not*I sites of pADT3T7tet for adenovirus generation. After PCR amplification, SNX9 cDNA was subcloned into *Hin*dIII/*Not*I sites of pADT3T7tet and into *Hin*dIII/*Xma*I sites of pEGFP-C3. SH3(SNX9) cDNA was amplified by PCR and subcloned into the *Bam*HI/*Eco*RI sites of pGEX.KG. C-terminally-tagged dynamin-1 mRFP (designated pmRFP-N1-dyn 1) was generated by replacing EGFP with mRFP in pEGFP-N1-dyn 1 (Song *et al.*, 2004) using *Age*I and *Not*I.

For generation of recombinant adenoviruses, wild-type HA-SNX9 cDNA was cloned into pADT3T7tet vector. HEK293-Cre cells were transfected with pADTetT3T7 vectors and adenoviruses were produced as described (Hardy *et al.*, 1997).

Antibodies

Anti-SNX9 rabbit polyclonal antibodies were generated in female New Zealand White rabbits immunized with full-length SNX9 fused to GST and purified from *Escherichia coli*. Antibodies were affinity-purified against the antigen. The monoclonal antihemagglutinin-tag antibody, 12CA5, was provided by I. Wilson (The Scripps Research Institute, La Jolla, CA). Monoclonal anti-β-tubulin and monoclonal anti-Golgi 58K protein antibodies were obtained from Sigma (St. Louis, MO). Monoclonal antidynamin, Hudy-1, was generated in this laboratory (Warnock *et al.*, 1995). Monoclonal anticlathrin, X22, was provided by F. Brodsky (University of California, San Francisco, CA).

Immunoprecipitation and Cellular Extracts

HA-dynamin-1 or HA-dynamin-2 were overexpressed by infection of tTA HeLa cells with recombinant adenoviruses (Altschuler *et al.*, 1998). Total cell extract was obtained by incubating cells for 5 min in cold lysis buffer (50 mM Tris, pH 8.0, 1% NP40) and spinning the lysate in a microfuge at 14,000 rpm 5 min at 4°C. Supernatant was used as total cell extract. Three cycles of freezing/thawing of cells in buffer A (0.25 M sucrose, 1 mM $MgCl_2$, 2 mM EGTA, and 25 mM HEPES, pH 7.4) and spinning at 100,000 × *g* for 30 min at 4°C gave the membrane enriched fraction (pellet) and the complementary cytosol (supernatant).

For anti-HA immunoprecipitations, after preclearing with protein-G dynabeads and nonspecific antibody, extracts were incubated with 5 μg of antibodies for an hour at 4°C. Magnetic protein-G dynabeads were then added for an additional 30 min. After extensive washes with lysis buffer, proteins bound to the beads were subjected to SDS-PAGE and Western blot analysis. For antidynamin-2 immunoprecipitations, a similar protocol was used except that the antibody specific for dynamin (Hudy-1) was prebound to protein-G dynabeads before incubation with cell extracts to improve the yield of the immunoprecipitation.

Protein Expression and Pull-down Assay

Wild-type and mutant dynamins were expressed and purified as previously described (Song *et al.*, 2004). The human amphiphysin-I GST fusion construct (GST-amph1) was obtained from Pietro DeCamilli (Yale University) and purified using GST-Sepharose by standard protocols. Wild-type and mutant SNX9 were expressed as GST-fusion proteins in BL21 *E. coli* strain after induction with 0.1 mM isopropyl β-D-thiogalactoside at 30°C for 2 h in LB medium + ampicillin. Pellets of bacteria were resuspended in phosphate-buffered saline (PBS) plus protease inhibitor cocktail (Sigma). After lysozyme treatment for 5 min, cells were sonicated then incubated 10 min at 4°C with 1 mg of DNase and 10 mM $MgCl_2$. After addition of Triton X-100–1% final concentration, lysates were incubated for 10 min at 4°C and then spun at 3000 × *g* for 10 min. The supernatant was subjected to affinity purification using glutathione-Sepharose 4B beads (Amersham Bioscience, Piscataway, NJ) according to the manufacturer's instructions.

For pull-down experiments, 2.5 μg of GST fusion protein was bound to 10 μl of glutathione-Sepharose beads. The loaded beads were incubated with 2.5 μg of purified dynamin for 1 h at 4°C on a roller in a final volume of 500 μl of lysis buffer. After three washes (500 μl), beads were transferred to a new tube and the bound proteins were analyzed by SDS-PAGE followed by Coomassie-blue staining.

Immunofluorescence

For indirect immunofluorescence, HeLa cells cultured overnight on poly-L-lysine–coated coverslips were fixed for 15 min in formaldehyde 4%. Cells were permeabilized with PBS containing 0.1% Triton X-100 and 2% bovine serum albumin and stained with different primary antibodies (monoclonal anticlathrin, X22; monoclonal antidynamin, hudy-1; and polyclonal anti-SNX9) followed by Alexa 488–conjugated anti-rabbit and rhodamine-conjugated anti-mouse secondary antibodies (Molecular Probes, Eugene, OR). Images were either obtained by wide-field epifluorescence microscopy using a Olympus BX-50WI microscope (Lake Success, NY) equipped with a C4742–95 camera (Hamamatsu, Bridgewater, NJ) or by confocal microscopy using an Olympus Fluoview 500.

Fluorescence Videomicroscopy

For EGFP-SNX9 and CLC-DsRed experiments, Swiss 3T3 cells stably expressing clathrin-light chain DsRed (kindly provided by W. Almers, Vollum Institute, Oregon Health and Sciences University) were grown to 70% confluency in a 100-mm tissue culture dish in DMEM + 10% fetal calf serum and transfected with 20 μg EGFP-SNX9 DNA using Lipofectamine 2000 (Invitrogen, Carlsbad, CA) according to manufacturer's instructions. Cells were allowed to recover in fresh medium for 2 h, replated onto 22 × 22-mm, no. 1.5 glass coverslips (Corning, Corning, NY, n = 1.523), and filmed the following morning. For EGFP-SNX9 and dynamin 1-mRFP experiments, Swiss 3T3 cells were plated onto glass coverslips and allowed to adhere overnight. Cells were microinjected with plasmids encoding EGFP-Snx9 (0.05 mg/ml) and Dynamin1-mRFP (0.05 mg/ml) into the nucleus 3–5 h before filming.

Nearly simultaneous total internal reflection fluorescence (TIRF) and wide-field epifluorescence (WF-EF) microscopy was performed using an inverted microscope (Nikon TE2000U, Melville, NY) custom-modified to allow for through-the-objective multispectral total-internal reflection fluorescence microscopy and wide-field epifluorescence (Adams *et al.*, 2004) using a 100×, 1.45 NA objective (Nikon), as previously described (Yarar *et al.*, 2005). Pairs of WF-EF and TIRF images were taken for 10 min at 2–3-s intervals, with 100–300-ms exposure time, depending on the intensity of the signal.

GTPase and Sedimentation Assay

GTP hydrolysis was measured at 200 μM GTP using a colorimetric assay to detect P_i release as previously described (Song *et al.*, 2004) in the presence or absence of $PI4,5P_2$-containing liposomes. To prepare liposomes, 76 μl of a 10 mg/ml stock of egg yolk phosphatidyl choline (Calbiochem, La Jolla, CA) in chloroform was mixed with 110 μl of 1 mg/ml stock of porcine brain $PI_{4/5}P_2$ (Avanti Polar Lipids, Birmingham, AL). Chloroform was evaporated under nitrogen and the lipids were resuspended in 2.5 ml 50 mM HEPES, pH 7.5, and 150 mM KCl. Aliquots, 250 μl, were taken through five cycles of freeze-thaw (thawing at 37°C) and vortexing before storage at −80°C for up to 12 mo. Lipid solutions were thawed and extruded through 0.4-μm polycarbon-

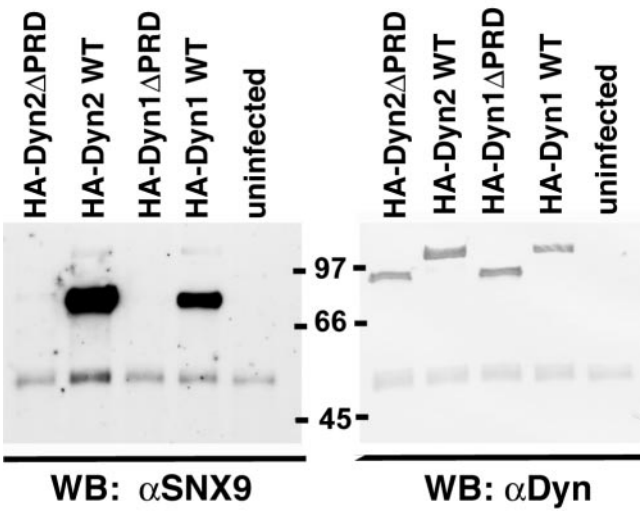

Figure 1. SNX9 interacts in vivo with dynamin-1 and dynamin-2. tTA-HeLa cells were untreated or infected with recombinant adenoviruses encoding HA-dynamin-2ΔPRD, HA-dynamin-2, HA-dynamin-1ΔPRD, and HA-dynamin-1. Total extracts were immunoprecipitated with the anti-HA antibody, 12CA5. The immunoprecipitated proteins were analyzed by immunoblot sequentially using polyclonal α-SNX9 antibodies and anti-HA antibodies.

ate filters under pressure using an Avanti Extruder apparatus and stored at 4°C. Liposomes were used within 1 wk of preparation.

For the velocity sedimentation assays, dynamin (2 μM) was incubated 10–20 min at room temperature in the GTPase assay buffer (10 mM HEPES, pH 7.2, 2 mM $MgCl_2$, 150 mM KCl) with increasing amounts of GST-SNX9 or GTP-amph1. The reaction mixture (50 μl) was centrifuged for 10 min at 14,000 rpm in a microfuge at 4°C. Equal volumes of the pellet and supernatant fractions were analyzed by SDS-PAGE followed by Coomassie blue staining.

siRNA Treatment and Endocytosis Assays

siRNA treatments were performed according to established protocols (Elbashir *et al.*, 2002) except that oligofectamine (Invitrogen) was used as a delivery agent. Briefly, HeLa cells were plated the day before at 30–40% confluency and transfected with 60 μl of siRNA oligos (20 μM, Qiagen, Chatsworth, CA) that target the following sequence for SNX9: AACAGTCGTGCTAGTTCCTCA, and for the control: AATTCTCCGAACGTGTCACGT, in Optimem medium. After 3–5 h, the medium was supplemented with FCS to being the final concentration up to 10%. Cells were incubated for 48 h and then passed for a low confluence. After a further 24 h, TfnR uptake was determined as previously described (van der Bliek *et al.*, 1993). Internalization of ^{125}I-epidermal growth factor was determined as previously described (Conner and Schmid, 2003).

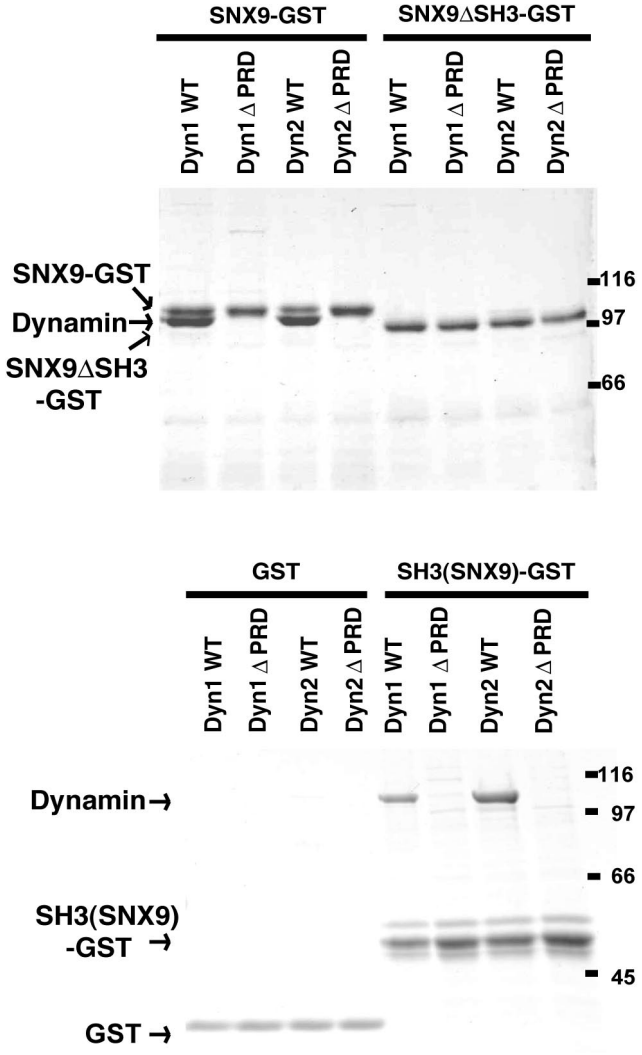

Figure 2. SNX9 interacts directly with dynamin in vitro. The GST fusion proteins, GST-SNX9, GST-SNX9ΔSH3, GST-SH3(SNX9), or GST alone were immobilized on glutathione-Sepharose-beads and incubated with purified dynamin-1, dynamin-1ΔPRD, dynamin-2, or dynamin-2ΔPRD as described in *Materials and Methods.* Bound proteins were then analyzed by SDS-PAGE and Coomassie blue staining.

RESULTS

SNX9 Interacts Directly with Both Dynamin-1 and Dynamin-2

To identify dynamin binding partners in vivo, hemagglutinin (HA)-epitope tagged dynamin-1 was overexpressed in HeLa cells and immunoprecipitated from total cell lysate using an anti-HA antibody. Coimmunoprecipitated proteins were detected by silver-stain after SDS-gel electrophoresis (unpublished data). A prominent band migrating at ~70 kDa was excised and digested, and the peptides were subjected to tandem mass spectroscopy. The protein was identified as sorting nexin 9, SNX9. We confirmed the SNX9-dynamin interaction using SNX9-specific antibodies and found by Western blot analysis that SNX9 efficiently coimmunoprecipitated with both HA-tagged dynamin-1 and dynamin-2 (Figure 1) from whole-cell lysates. However SNX9 did not coimmunoprecipitate with HA-tagged dynamin-1ΔPRD or dynamin-2ΔPRD deletion mutants that lack the C-terminal pro/arg-rich domain (Figure 1). We conclude that the SNX9 interaction in vivo is mediated by dynamin's PRD.

We further characterized the dynamin-SNX9 interactions using GST-tagged full-length SNX9, truncated SNX9 lacking its N-terminal SH3 domain (SNX9ΔSH3) and the SNX9 SH3 domain alone (SH3(SNX9)) expressed in and purified from *E. coli*. The GST-SNX9 fusions and GST were immobilized on glutathione-Sepharose beads. Recombinant purified full-length dynamin-1 and dynamin-2, but not dynamin-1ΔPRD nor dynamin-2ΔPRD, bound directly to both GST-SNX9 and GST-SH3(SNX9) (Figure 2). However, dynamin proteins did not interact with GST or with GST-SNX9ΔSH3 (Figure 2). These studies show that SNX9 interacts with both dynamin-2 and dynamin-1 and that this interaction is mediated by the PRD of dynamin and the SH3 domain of SNX9.

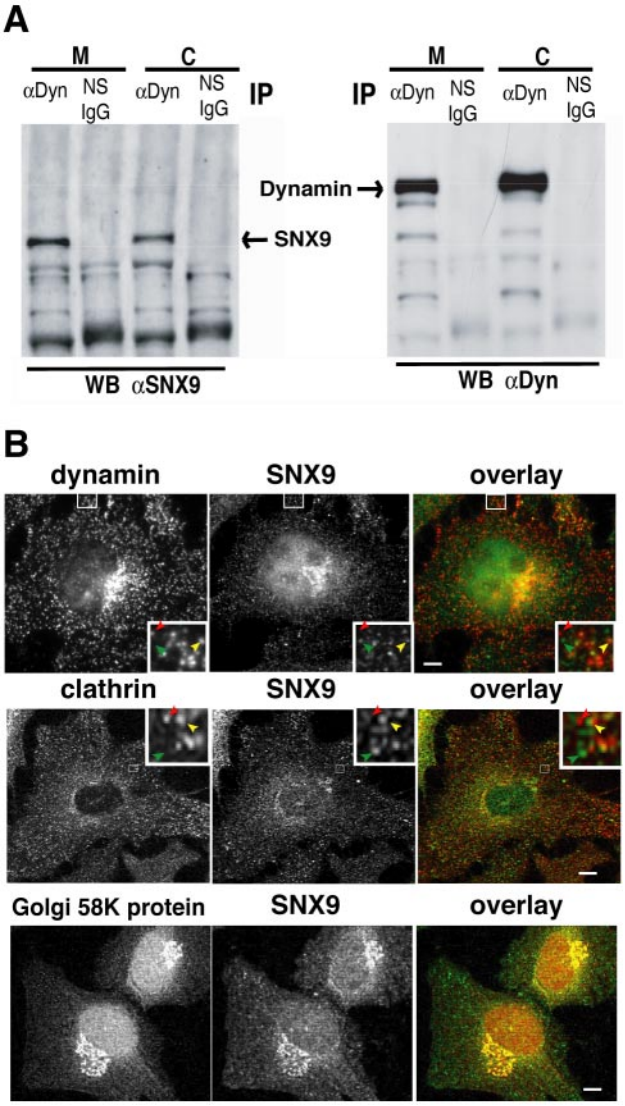

Figure 3. SNX9 interacts with dynamin and clathrin at the plasma membrane. (A) tTA-HeLa cells were fractionated into membrane enriched (M) or cytosolic fractions (C). Each fraction was separately immunoprecipitated with a monoclonal antidynamin antibody, Hudy-1 or a nonspecific mouse antibody (NS IgG). The immunoprecipitated proteins were analyzed by sequential immunoblot using anti-SNX9 antibody followed by antidynamin polyclonal antibody (4003). (B) Indirect immunofluorescence in HeLa cells of SNX9 (green) shows partial colocalization with dynamin-2 and clathrin. Inset: higher magnification of the indicated area. Red arrows: pits without SNX9; green arrows: pits with only SNX9; yellow arrows: colocalization. SNX9 also colocalizes with the Golgi marker, Golgi p58 protein. Scale bar, 10 μm.

SNX9 and Dynamin Interact at the Plasma Membrane

Dynamin plays a fundamental role in endocytosis and exists in the cytosol and at the plasma membrane where it is concentrated at CCPs (van der Bliek *et al.*, 1993). To determine whether dynamin-SNX9 interactions occur with both pools of dynamin, HeLa cells were lysed by freeze-thaw cycles and the total membrane fraction was separated from the cytosolic fraction by sedimentation. Endogenous SNX9 was efficiently coimmunoprecipitated with endogenous dynamin-2 from both fractions. However, we found that the ratio of SNX9:dynamin coimmunoprecipitating from the membrane fraction appeared to be greater than from the cytosolic fraction (Figure 3A). These data suggest that SNX9-dynamin interactions may be enhanced at the membrane.

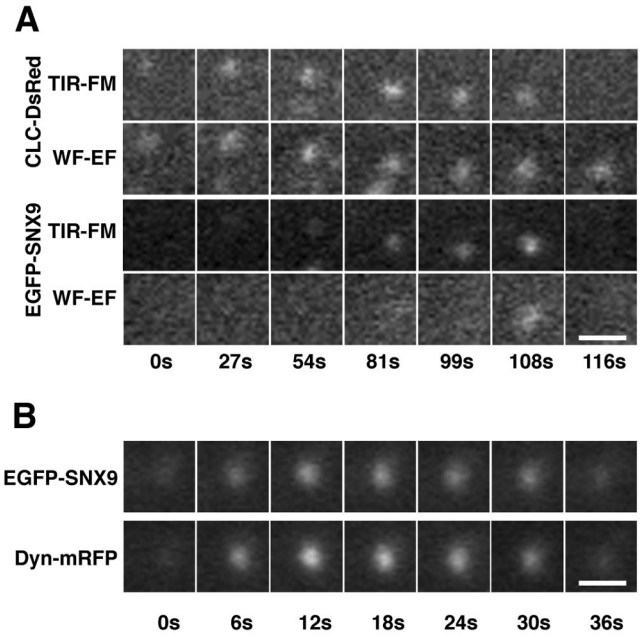

Figure 4. SNX9 is transiently recruited to clathrin-coated pits late in coated vesicle formation. Images from time-lapse sequences showing the behavior of (A) CLC-DsRed and EGFP-SNX9 imaged by TIR-FM and WF-EF (see also Supplementary Movies 1 and 2) and (B) EGFP-SNX9 and dynamin1-mRFP imaged by TIR-FM (see also Supplementary Movie 3). Scale bar, 1 μm.

SNX9 Is Transiently Recruited, at a Late Stage, to Coated Pits

We next immunolocalized SNX9 in HeLa cells relative to clathrin and dynamin. SNX9 partially colocalized with both clathrin and dynamin (Figure 3B) in punctate structures at the cell surface and in the perinuclear region. Colocalization with Golgi 58K protein, a marker for the Golgi apparatus and of TGN-derived vesicles (Hennig *et al.*, 1998), confirmed that SNX9 is also associated with this organelle (Figure 3B). Localization of SNX9 to the Golgi and TGN, as well as the plasma membrane, is consistent with the ability of SNX9 to interact with the appendage domains of both α- and γ-adaptins (Hirst *et al.*, 2003).

The partial colocalizations of SNX9 with plasma membrane-associated CCPs (inset, Figure 3B) may reflect either the association of SNX9 with a select subpopulation of CCPs or the transient interactions of SNX9 with all CCPs. To distinguish between these possibilities, we examined the dynamic interaction of transiently transfected EGFP-SNX9 with plasma membrane–associated coated pits in living cells stably expressing clathrin light chain-DsRed (CLC-DsRed). Overexpression of SNX9 has no effect on transferrin (Tfn) endocytosis (see below). Live cells were imaged using total internal reflection fluorescence microscopy (TIR-FM) and near-simultaneous wide field epifluorescence microscopy (WF-EF; Supplementary Movie 1). Strikingly, we observed a transient burst of EGFP-SNX9 localization to endocytic CCPs that occurred during late stages of clathrin-coated vesicle formation (Figure 4A, Supplementary Movie 2). The

transient increase in EGFP-SNX9 fluorescence was observed both by TIR-FM and by WF-EF, reflecting the late recruitment of SNX9 to coated pits rather than its redistribution closer to the plasma membrane. There was some variability in the spatial and temporal relationship between SNX9 and clathrin. Although SNX9 and clathrin foci were always spatially overlapping, and most were centered or became centered with time (82%, 36 of 44 events), the remainder were off-center or became off-center through time. Interestingly, large SNX9 structures could sometimes be detected emerging from the side of a CCP (see Supplementary Movie 1). At this time resolution (2–3 s/frame), the peak of the SNX9 burst was observed to occur either just before (15%, 3 of 20 events), coincident with (55%, 11 of 20 events), or just after (30%, 6 of 20 events) the selective disappearance of DsRed-CLC fluorescence from TIR-FM; although in some cases (~15%, 7 of 48 events) CCP internalization could be observed independent of a SNX9 burst.

The kinetics of SNX9 recruitment to CCPs were reminiscent of those observed by others for dynamin-EGFP (Merrifield *et al.*, 2002). This relationship was more closely examined by simultaneously following EGFP-SNX9 and dynamin-1-mRFP dynamics by TIR-FM. Although we could detect cases where EGFP-SNX9 and dynamin-1-mRFP fluorescence increased independently, in the majority of cases (65%, 15 of 23 events) the kinetics of increase and decrease in fluorescence intensity at the cell surface were indistinguishable (Figure 4B, Supplementary Movie 3). We also detected increases in dynamin-1-mRFP fluorescence independent of SNX9 (unpublished data), which could represent dynamin recruitment to other endocytic structures. These data suggest that SNX9 and dynamin are transiently recruited to endocytic CCPs at a late stage of clathrin-coated vesicle (CCV) formation.

SNX9 Stimulates Dynamin's Basal GTPase Activity

Our results and those of others (Lundmark and Carlsson, 2004) establish that SNX9 interacts with dynamin in vivo during clathrin-mediated endocytosis. To determine whether this interaction regulates aspects of dynamin activity in vitro, we first measured dynamin's basal rate of GTP hydrolysis in the presence or absence of GST-SNX9 (Figure 5A). GST-SNX9 stimulated the basal GTPase activities of both dynamin-1 (▲, △) and dynamin-2 (■, □; Figure 5A). Stimulation by GST-SNX9 was concentration-dependent and maximal stimulation, about sevenfold, was obtained at a 2:1 stoichiometry of SNX9:dynamin (Figure 5B, ▲). As expected, GST-SNX9ΔSH3 was unable to stimulate dynamin's GTPase activity (Figure 5B, △). Interestingly, although the SH3 domain of SNX9 was sufficient for dynamin binding, GST-SH3(SNX9) did not stimulate dynamin's GTPase activity (Figure 5B, ○). This result suggests that other features of full-length SNX9 are required to stimulate dynamin.

To further probe the specificity of the SNX9 stimulation, we compared SNX9 activation of dynamin's GTPase activity with another SH3 domain-containing dynamin binding partner, amphiphysin-1. Like SNX9, amphiphysin-1, also binds clathrin and AP2, has a coiled-coil domain, a proline-rich region, and a BAR domain involved in lipid binding and dimerization (Zhang and Zelhof, 2002). Nonetheless, we find that, under our assay conditions and at physiological salt concentrations, neither full-length GST-amphiphysin-1 (GST-amph1) nor its SH3 domain, GST-SH3(amph), stimulate dynamin's basal GTPase activity (Figure 5B, ■ and □, respectively).

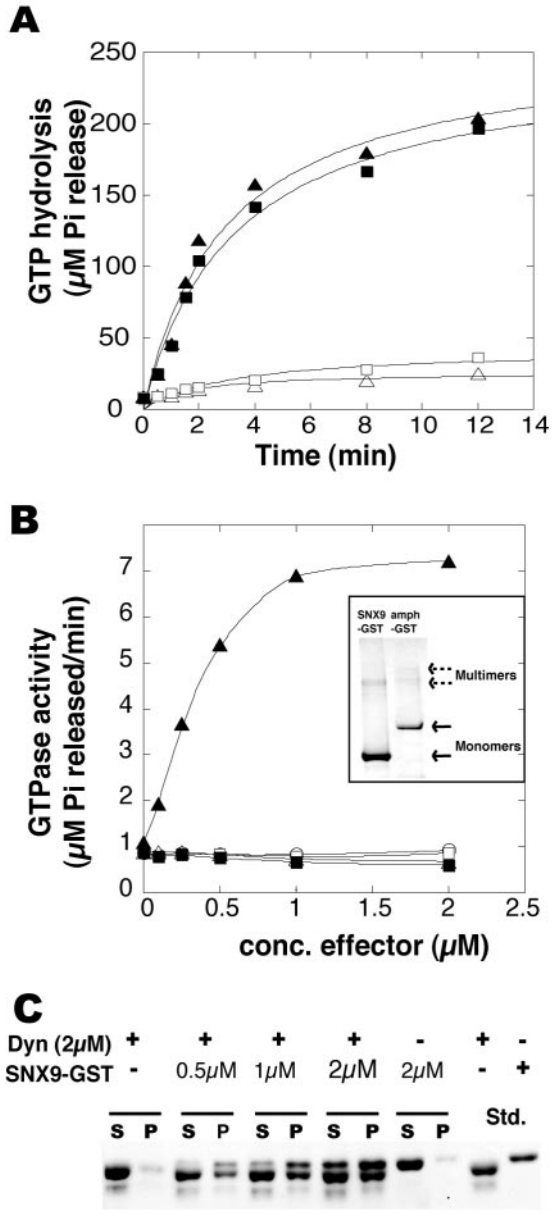

Figure 5. SNX9 stimulates dynamin basal GTPase activity. The basal rate of GTP hydrolysis was measured at high salt concentration (150 mM KCl) and 0.5 μM dynamin. (A) The amount of Pi released by dynamin-1 (▲, △) or dynamin-2 (■, □) in the presence (closed symbols) or absence (open symbols) of 1 μM GST-SNX9, is plotted as a function of time. (B) Rate of GTP hydrolysis by dynamin-1 was measured and plotted as a function of increasing concentrations of effector: GST-SNX9 (▲), GST-SNX9ΔSH3 (△), and GST-SH3(SNX9) (○), GST-amph1 (■), and GST-SH3(amph) (□). (C) Self-assembly of dynamin-1 was examined by velocity sedimentation at physiological salt concentration (150 mM KCl), followed by SDS-PAGE analysis of the pellet (P) and supernatant (S).

Previous studies have shown that dynamin's basal GTPase activity can be stimulated by dynamin assembly induced by binding of polymers to its PRD (Warnock *et al.*, 1997; Barylko *et al.*, 1998). Thus, the differential effect of GST-SNX9 compared with GST-amph1, may reflect differential oligomerization of these proteins. We tested this hypothesis by chemical cross-linking, but found no difference

in the oligomerization state of GST-SNX9 compared with GST-amph1 (Figure 5B, inset). Thus, we conclude that SNX9 stimulates dynamin's GTPase activity and that the SH3 domain of SNX9 is necessary, but not sufficient for this regulation.

SNX9 Induces Dynamin Self-assembly

Stimulation of dynamin's GTPase activity could be accomplished either directly by enhancing basal GTP hydrolysis or indirectly by enhancing dynamin's ability to self-assemble. Thus, we next looked for stimulation of dynamin self-assembly by SNX9 using a cosedimentation assay. When incubated at physiological salt concentrations, dynamin alone will not self-assemble and therefore remains mostly in the supernatant after sedimentation (Figure 5C). Similarly, GST-SNX9 does not self-assemble into sedimentable structures (Figure 5C). However, when GST-SNX9 is incubated with dynamin, the two proteins coassemble into sedimentable structures that contain near stoichiometric amounts of dynamin and GST-SNX9 (Figure 5C). Consistent with their inability to stimulate GTPase activity, neither GST-SNX9ΔSH3, GST-SH3(SNX9), nor GST-amph1 were able to induce dynamin assembly under these assay conditions (unpublished data).

Snx9 and Liposomes Synergize to Enhance Dynamin's Assembly-stimulated GTPase

The assembly-stimulated GTPase activity of dynamin is maximally induced in the presence of ~50-nm diameter $PI4,5P_2$-containing lipid nanotubules (Marks *et al.*, 2001), and this is not further enhanced in the presence of SNX9 (unpublished data). Dynamin also self-assembles onto $PI4,5P_2$-containing liposomes generated by extrusion through 0.4-μm filters (Song *et al.*, 2004). However, the assembly-stimulated GTPase activity of dynamin on liposomes is lower than that on lipid nanotubules, reflecting, in part, its less efficient assembly on these templates. To determine whether SNX9 might enhance dynamin assembly onto liposomes, we examined dynamin's GTPase activity in the presence and absence of $PI4,5P_2$-containing liposomes (Figure 6A). In these assays, dynamin is present at low, more physiologically relevant concentrations (0.2 μM), has little detectable GTPase activity on its own (open circles, dashed line), and is only weakly stimulated in the presence of 4 μM $PI4,5P_2$-containing liposomes (●). As previously shown (Figure 5B), in the presence of equimolar concentrations GST-SNX9 (△) dynamin's GTPase activity in solution is stimulated about sixfold. In contrast, under these conditions GST-amph1 either at equimolar concentrations (□) or at fivefold molar excess (unpublished data) has no effect on dynamin's GTPase activity. Strikingly, when assayed in the presence of both liposomes and equimolar GST-SNX9, dynamin's assembly-stimulated GTPase activity was strongly enhanced (▲). In contrast GST-amph1 was, if anything, inhibitory (■ vs. ●), as has previously been reported (Owen *et al.*, 1998; Takei *et al.*, 1999). The synergistic effect of SNX9 and liposomes on dynamin's GTPase activity was highly reproducible (Figure 6B). Assembly of dynamin alone onto liposomes stimulated GTPase activity by about threefold, SNX9 alone stimulated dynamin's GTPase activity by about fivefold, and strikingly, when both SNX9 and liposomes were present, they acted synergistically to stimulate dynamin's GTPase activity by ~20-fold. Thus, SNX9 stimulates dynamin self-assembly and assembly-stimulated GTPase activity both in solution and onto liposomes.

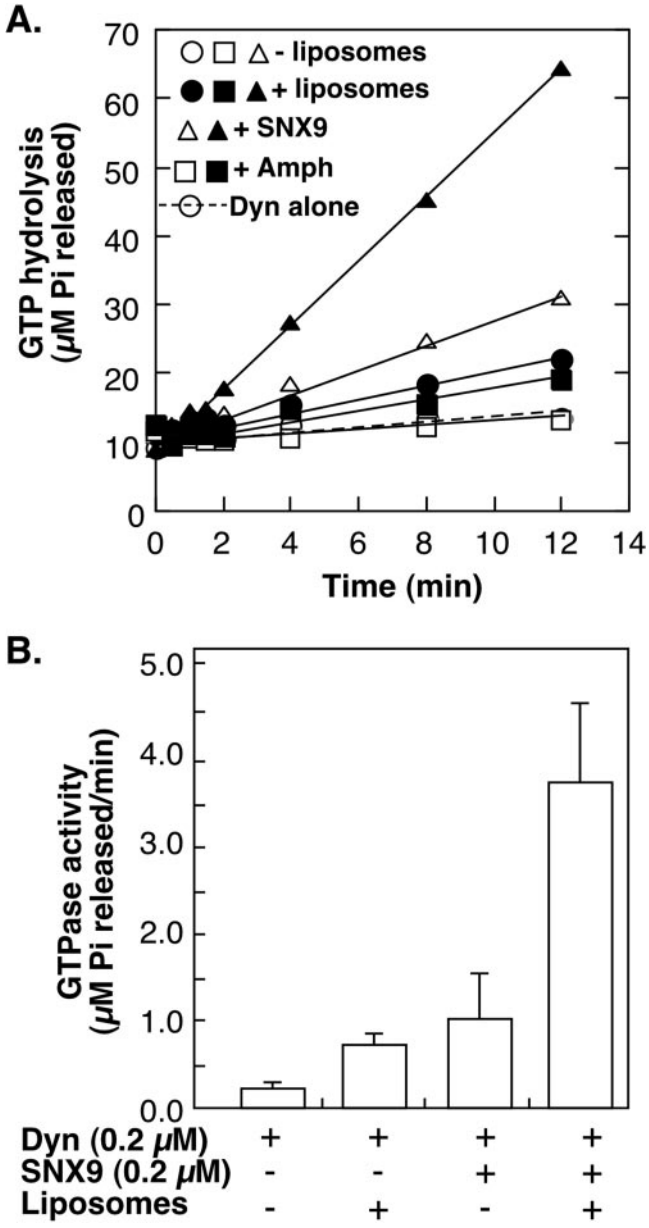

Figure 6. SNX9 and liposomes synergistically enhance dynamin's assembly-stimulated GTPase activity. (A) The GTPase activity of dynamin-1 (0.2 μM) was measured alone without (○, dashed line) or with (●) liposomes, or in the presence of 0.2 μM GST-SNX9 (△), 0.2 μM GST-SNX9 and liposomes (●), 0. 2 μM GST-amph1 (□), or 0.2 μM GST-amph1 and liposomes (■). Assays were performed as described in *Materials and Methods.* (B) Rates of GTP hydrolysis for dynamin-1 alone, with liposomes, with SNX9 and with SNX9 and liposomes, were measured in three independent experiments. Data shown are averages ± SD.

SNX9 Is Required for Transferrin Receptor Internalization

SNX9 binds to each of the key components of the clathrin-mediated endocytic machinery, namely clathrin, dynamin, and AP2 (Lundmark and Carlsson, 2002, 2003; Miele *et al.*, 2004). Others have shown that endocytosis is inhibited by overexpression of a C-terminal truncation mutant of SNX9 (Lundmark and Carlsson, 2003). However, because this construct retains the ability to bind clathrin, dynamin, and AP2, the observed dominant negative effect could be due to titra-

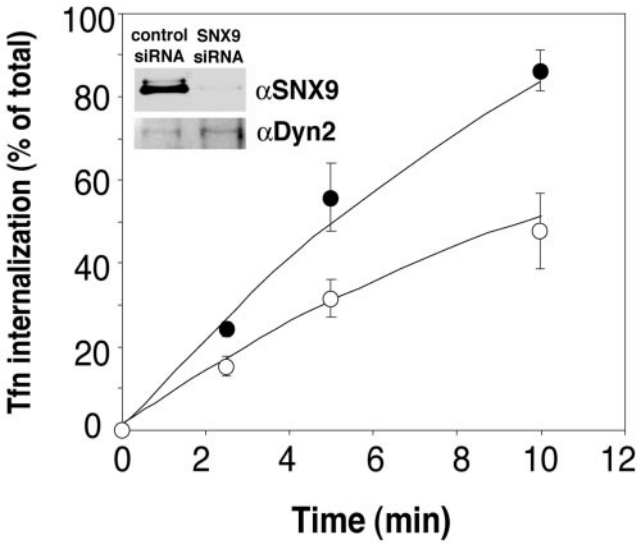

Figure 7. SNX9 is required for efficient TfnR internalization. HeLa cells were transfected with two different siRNA constructs, one targeting specifically SNX9 (siRNA-SNX9) and another nonsilencing (siRNA control). The inset is a Western blot showing that SNX9 expression and not dynamin-2 expression is selectively reduced in siRNA-SNX9 treated cells. After siRNA treatment, single round internalization assays show an inhibition of Tfn internalization with the siRNA-SNX9 measured 72 h after transfection with control (●) or SNX9 (○) siRNAs. The percentage of total surface bound Tfn internalized during incubation at 37°C is plotted as a function of time. Data are averages ± SD from three independent experiments.

tion of any of these essential components. Therefore, to determine whether SNX9 is required for endocytosis, we used small RNA-mediated gene silencing with small interfering RNA (siRNA) to knockdown SNX9 expression. HeLa cells were transfected with siRNAs that specifically target SNX9. After 72 h, SNX9 expression was reduced by ~90% compared with control cells treated with nonspecific siRNA: neither dynamin (inset, Figure 7) nor tubulin (unpublished data) expression levels were reduced. When receptor-mediated endocytosis of transferrin (Tfn) was measured, we found that the rate of Tfn uptake was inhibited by ~45% in siRNA-treated cells compared with control cells (Figure 7). A similar extent of inhibition was observed in preliminary experiments for uptake of ^{125}I-epidermal growth factor (unpublished data). From these results, we conclude that SNX9 is required for efficient clathrin-mediated endocytosis.

In addition to its SH3 domain, SNX9 has a PX domain that was reported to bind nonspecifically to different phosphatidylinositol-phosphate–containing liposomes, and a central region shown to bind AP2 and clathrin (Lundmark and Carlsson, 2003; Miele *et al.*, 2004). Given its multiple protein and lipid binding domains, SNX9 may function as a scaffold molecule. If so, then overexpression of SNX9 molecules unable to bind dynamin but able to bind lipids and other proteins should function as dominant-negative mutants. To test this hypothesis, we generated recombinant adenovirus expressing full-length SNX9 and SNX9ΔSH3. Surprisingly, neither wild-type SNX9 nor SNX9ΔSH3 inhibited endocytosis even when highly overexpressed (unpublished data). Together these data suggest that SNX9 is required for efficient endocytosis and that its function in vivo is dependent on dynamin binding.

DISCUSSION

We have shown that SNX9 is required for efficient TfnR-mediated endocytosis and provided in vivo and in vitro evidence to suggest that SNX9 functions to regulate dynamin self-assembly during late stages of endocytic vesicle formation. In vivo, using near simultaneous TIRF and WF-EF microscopy, we observe a transient burst of EGFP-SNX9 fluorescence at CCPs during late stages of CCV formation. EGFP-SNX9 fluorescence increased in parallel in the TIRF and WF-EF images, thus we conclude that it reflects the recruitment of EGFP-SNX9 from the cytosol. This burst occurred just before, coincident with, or just after the disappearance of DsRed-CLC from the TIR-FM image and was coincident with a transient increase in dynamin-mRFP fluorescence at CCPs observed by TIR-FM. A burst of dynamin fluorescence before CCV formation was reported in earlier studies (Merrifield *et al.*, 2002); however, it was unclear whether the increase in fluorescence reflected de novo recruitment, redistribution, or both. Indeed, EM immunolocalization studies (Damke *et al.*, 1994; Warnock *et al.*, 1997; Evergren *et al.*, 2004) and more recent analysis by confocal microscopy reporting the coincident recruitment of EGFP-dynamin and mRFP-clathrin to nascent coated pits (Ehrlich *et al.*, 2004) have established that dynamin is present at early stages of CCV formation. Thus, the increase in intensity of EGFP-dynamin fluorescence seen late in CCV formation may reflect the redistribution of this CCP-associated pool of dynamin closer to the membrane, the recruitment of additional dynamin from the cytosol, or both. The lack of contrast in our WF-EF images of EGFP-dynamin fluorescence precludes us from unambiguously determining whether the increased dynamin fluorescence represents recruitment. Given that SNX9-dynamin complexes are prevalent in the cytosol (Lundmark and Carlsson, 2003), we cannot exclude the possibility that these are recruited earlier to CCPs, but at levels below detection. Nonetheless, our data strongly suggest that SNX9-dynamin complexes are recruited de novo, late in CCV formation.

Amphiphysin and SNX9 are structurally similar molecules and share common binding partners (Wigge and McMahon, 1998; Di Paolo *et al.*, 2002; Zhang and Zelhof, 2002; Lundmark and Carlsson, 2002, 2003). Both have SH3 domains and BAR domains, and both proteins bind dynamin, AP2, clathrin, and lipids. Finally, both have been implicated in regulation of the actin cytoskeleton (Mundigl *et al.*, 1998; Worby *et al.*, 2001). Thus, it has been suggested that SNX9, like amphiphysin, might function as an endocytic scaffold to recruit dynamin to the plasma membrane as CCPs assemble (Lundmark and Carlsson, 2004). Such a model is supported by recent evidence that SNX9 can stimulate dynamin binding to cellular membranes in vitro (Lundmark and Carlsson, 2004). Our findings suggest that SNX9-dynamin complexes are recruited late in CCV formation where they coassemble at the necks of deeply invaginated coated pits and we propose that other factors function to recruit dynamin to CCPs during early stages of coated pit formation. This two-step model for recruitment of dynamin to CCPs is consistent with the findings that the punctate staining pattern of dynamin-2 on the plasma membrane is retained, albeit reduced in SNX9-deficient cells (Lundmark and Carlsson, 2004) and that the electron-dense collars observed by conventional thin-section EM may contain other proteins in addition to dynamin (Takei *et al.*, 1999).

Several lines of evidence from the work presented here and results of others suggest that amphiphysin and SNX9 have distinct functions in clathrin-mediated endocytosis.

First, we see a clear defect in Tfn uptake upon SNX9 knockdown, suggesting that endogenous amphiphysin cannot substitute for loss of SNX9 activity and that SNX9 is required for efficient clathrin-mediated endocytosis. In contrast, although some aspects of synaptic vesicle recycling were perturbed in amphiphysin-deficient mice, no defect in the kinetics of synaptic vesicle endocytosis could be detected (Di Paolo *et al.*, 2002), and there was no defect in synaptic function in amphiphysin deficient *Drosophila* or *C. elegans* (Zhang and Zelhof, 2002). Second, we do not see an effect on Tfn uptake of overexpression of either wild-type SNX9 or SNX9ΔSH3 mutants defective in binding dynamin. If SNX9 functioned as a scaffold connecting clathrin, AP2, lipids, and dynamin, then we would expect, as has been observed with amphiphysin (Wigge *et al.*, 1997), that SNX9 mutants lacking the ability to bind dynamin, but retaining their ability to bind AP, clathrin, and lipids would compete with endogenous SNX9 when overexpressed and result in dominant interference of endocytosis. Importantly, overexpression of the SH3 domain-containing fragments of both amphiphysin (Wigge *et al.*, 1997; Owen *et al.*, 1998), and SNX9 (Lundmark and Carlsson, 2003) inhibit Tfn uptake, supporting the in vivo importance of their interactions with dynamin. Finally, we have shown that SNX9, but not amphiphysin, stimulates dynamin self-assembly in solution and onto small (<400 nm) PI4,5P_2-containing liposomes. Indeed we and others (Owen *et al.*, 1998; Takei *et al.*, 1999; Yoshida *et al.*, 2004) have shown that amphiphysin, if anything, inhibits dynamin self-assembly onto small PI4,5P_2-containing liposomes. Thus, SNX9 and amphiphysin, although structurally related, are functionally distinct dynamin binding partners.

Dynamin interacts with numerous functionally diverse SH3 domain-containing partners, which we have proposed might function as effector molecules mediating distinct stages in CCV formation (Song *et al.*, 2003). In this regard, a recent report showing that amphiphysin can stimulate dynamin assembly and GTPase activity onto very large (>1.5 μM) unilamellar liposomes (Yoshida *et al.*, 2004) is of great interest. We speculate that membrane curvature might play a role in determining the hierarchy of interactions between dynamin and its effectors. Thus, amphiphysin might preferentially interact with dynamin on shallow CCPs at earlier stages of CCV formation (mimicked by large diameter liposomes), where it might inhibit self-assembly, whereas SNX9 might sense more highly curved CCPs (mimicked by small diameter liposomes) and function during the late stages of CCV formation to stimulate dynamin self-assembly. Further experimentation is needed to directly test this hypothesis.

We observed some heterogeneity in the temporal relationship of SNX9 with CCPs. In the majority of cases the peak of SNX9 recruitment coincided with the selective loss of clathrin from the TIR-FM images; however, we also detected SNX9 recruitment just before or just after CCV formation. In addition EGFP-SNX9 fluorescence was detected, in some cases, off-centered from clathrin. This spatial and temporal heterogeneity, which has also been observed for actin's association with CCPs (Yarar *et al.*, 2005), may reflect a dual role for SNX9 in endocytosis. In this regard, it is interesting that SNX9 has been shown to interact with WASP in *Drosophila* (Worby *et al.*, 2001). We did not detect gross differences in phalloidin staining of the actin cytoskeleton in control versus SNX9 siRNA-treated cells (unpublished data). However, further work will be needed to determine whether, in addition to regulating dynamin assembly, SNX9 might also play a role in regulating actin assembly, which also occurs late in CCV formation (Merrifield *et al.*, 2002).

Finally, we also detect SNX9 at the Golgi, and SNX9 has been shown to interact with both the AP2 and AP1 adaptors, through the appendage domains of the α- and γ-adaptins, respectively (Hirst *et al.*, 2003). These data suggest that it may be a general regulator of dynamin function. Dynamin is involved in the formation of a subset of vesicles from the TGN, for example, those transporting p75 to the apical surface in MDCK cells (Kreitzer *et al.*, 2000). It would be interesting to determine whether SNX9 might also be required for a subset of transport events at the TGN.

A functional link between a sorting nexin family member and a dynamin family member has also been demonstrated in yeast (Ekena and Stevens, 1995). Although there is no true dynamin orthologue in yeast, the dynamin family member, Vps1p, which is not conserved in mammalian cells, functions in membrane trafficking from the Golgi to the vacuole (Rothman *et al.*, 1990). Although its exact function has yet to be defined, Vps1p has been localized to the yeast Golgi (Wilsbach and Payne, 1993). Interestingly, the only gene identified in a suppressor screen for Vps1 mutants encoded Mvp1p, another member of the sorting nexin family (Ekena and Stevens, 1995). Thus, SNX9 may play a more general role in regulating dynamin assembly late in vesicle formation.

ACKNOWLEDGMENTS

We thank Quiong Lin and Wannian Yang for providing SNX9 cDNA, Carl Blobel for providing truncated constructs of SNX9 and anti-SNX9 polyclonal antisera. Scott Anderson in John Yates' laboratory performed the mass spectroscopy and Clare Waterman-Storer provided instrumentation and assistance in the live cell fluorescence microscopy. This work was supported by National Institutes of Health grants GM42455 and MH61345 to S.L.S. and an American Cancer Society Fellowship PF-04-105-01-CSM to D.Y. We thank members of the Schmid laboratory for helpful discussions. This is TSRI Manuscript No. 16893-CB.

REFERENCES

Adams, M. C., Motov, A., Yarar, D., Gupton, S. L., Danuser, G., and Waterman-Storer, C. M. (2004). Signal analysis of total internal reflection fluorescent speckle microscopy (TIR-FSM) and wide-field epifluorescence FSM on the actin cytoskeleton and focal adhesions in living cells. J. Microscopy *216*, 138–152.

Altschuler, Y., Barbas, S. M., Terlecky, L. J., Tang, K., Hardy, S., Mostov, K. E., and Schmid, S. L. (1998). Redundant and distinct functions for dynamin-1 and dynamin-2 isoforms. J. Cell Biol. *143*, 1871–1881.

Barylko, B., Binns, D., Lin, K. M., Atkinson, M. A., Jameson, D. M., Yin, H. L., and Albanesi, J. P. (1998). Synergistic activation of dynamin GTPase by Grb2 and phosphoinositides. J. Biol. Chem. *273*, 3791–3797.

Cao, H., Thompson, H. M., Krueger, E. W., and McNiven, M. A. (2000). Disruption of Golgi structure and function in mammalian cells expressing a mutant dynamin. J. Cell Sci. *113*(Pt 11), 1993–2002.

Cheever, M. L., Sato, T. K., de Beer, T., Kutateladze, T. G., Emr, S. D., and Overduin, M. (2001). Phox domain interaction with PtdIns(3)P targets the Vam7 t-SNARE to vacuole membranes. Nat. Cell Biol. *3*, 613–618.

Conner, S. D., and Schmid, S. L. (2003). Differential requirements of AP-2 in clathrin-mediated endocytosis. J. Cell Biol. *162*, 773–779.

Cook, T. A., Urrutia, R., and McNiven, M. A. (1994). Identification of dynamin 2, an isoform ubiquitously expressed in rat tissues. Proc. Natl. Acad. Sci. USA *91*, 644–648.

Damke, H., Baba, T., Warnock, D. E., and Schmid, S. L. (1994). Induction of mutant dynamin specifically blocks endocytic coated vesicle formation. J. Cell Biol. *127*, 915–934.

Di Paolo, G. *et al.* (2002). Decreased synaptic vesicle recycling efficiency and cognitive deficits in amphiphysin 1 knockout mice. Neuron *33*, 789–804.

Ehrlich, M., Boll, W., Van Oijen, A., Hariharan, R., Chandran, K., Nibert, M. L., and Kirchhausen, T. (2004). Endocytosis by random initiation and stabilization of clathrin-coated pits. Cell *118*, 591–605.

Ekena, K., and Stevens, T. H. (1995). The *Saccharomyces cerevisiae* MVP1 gene interacts with VPS1 and is required for vacuolar protein sorting. Mol. Cell. Biol. *15*, 1671–1678.

Elbashir, S. M., Harborth, J., Weber, K., and Tuschl, T. (2002). Analysis of gene function in somatic mammalian cells using small interfering RNAs. Methods *26*, 199–213.

Evergren, E., Tomilin, N., Vasylieva, E., Sergeeva, V., Bloom, O., Gad, H., Capani, F., and Shupliakov, O. (2004). A pre-embedding immunogold approach for detection of synaptic endocytic proteins in situ. J. Neurosci. Methods *135*, 169–174.

Farsad, K., Ringstad, N., Takei, K., Floyd, S. R., Rose, K., and De Camilli, P. (2001). Generation of high curvature membranes mediated by direct endophilin bilayer interactions. J. Cell Biol. *155*, 193–200.

Fish, K. N., Schmid, S.L., and Damke, H. (2000). Evidence that dynamin-2 functions as a signal-transducing GTPase. J. Cell Biol. *150*, 145–154.

Gout, I. *et al.* (1993). The GTPase dynamin binds to and is activated by a subset of SH3 domains. Cell *75*, 25–36.

Gray, N. W., Fourgeaud, L., Huang, B., Chen, J., Cao, H., Oswald, B. J., Hemar, A., and McNiven, M. A. (2003). Dynamin 3 is a component of the postsynapse, where it interacts with mGluR5 and Homer. Curr. Biol. *13*, 510–515.

Habermann, B. (2004). The BAR-domain family of proteins: a case of bending and binding? EMBO Rep. *5*, 250–255.

Hardy, S., Kitamura, M., Harris-Stansil, T., Dai, Y., and Phipps, M. L. (1997). Construction of adenovirus vectors through Cre-lox recombination. J. Virol. *71*, 1842–1849.

Hennig, D., Scales, S. J., Moreau, A., Murley, L. L., De Mey, J., and Kreis, T. E. (1998). A formiminotransferase cyclodeaminase isoform is localized to the Golgi complex and can mediate interaction of trans-Golgi network-derived vesicles with microtubules. J. Biol. Chem. *273*, 19602–19611.

Hinshaw, J. E. (2000). Dynamin and its role in membrane fission. Annu. Rev. Cell. Dev. Biol. *16*, 483–519.

Hinshaw, J. E., and Schmid, S. L. (1995). Dynamin self-assembles into rings suggesting a mechanism for coated vesicle budding. Nature *374*, 190–192.

Hirst, J., Motley, A., Harasaki, K., Peak Chew, S. Y., and Robinson, M. S. (2003). EpsinR: an ENTH domain-containing protein that interacts with AP-1. Mol. Biol. Cell *14*, 625–641.

Howard, L., Nelson, K. K., Maciewicz, R. A., and Blobel, C. P. (1999). Interaction of the metalloprotease disintegrins MDC9 and MDC15 with two SH3 domain-containing proteins, endophilin I and SH3PX1. J. Biol. Chem. *274*, 31693–31699.

Kessels, M. M., Engqvist-Goldstein, A. E., Drubin, D. G., and Qualmann, B. (2001). Mammalian Abp1, a signal-responsive F-actin-binding protein, links the actin cytoskeleton to endocytosis via the GTPase dynamin. J. Cell Biol. *153*, 351–366.

Kranenburg, O., Verlaan, I., and Moolenaar, W. H. (1999). Dynamin is required for the activation of mitogen-activated protein (MAP) kinase by MAP kinase kinase. J. Biol. Chem. *274*, 35301–35304.

Kreitzer, G., Marmorstein, A., Okamoto, P., Vallee, R., and Rodriguez-Boulan, E. (2000). Kinesin and dynamin are required for post-Golgi transport of a plasma-membrane protein. Nat. Cell Biol. *2*, 125–127.

Lin, Q., Lo, C. G., Cerione, R. A., and Yang, W. (2002). The Cdc42 target ACK2 interacts with sorting nexin 9 (SH3PX1) to regulate EGF receptor degradation. J. Biol. Chem. *277*, 10134–10138.

Lundmark, R., and Carlsson, S. R. (2002). The beta-appendages of the four adaptor-protein (AP) complexes: structure and binding properties, and identification of sorting nexin 9 as an accessory protein to AP-2. Biochem. J. *362*, 597–607.

Lundmark, R., and Carlsson, S. R. (2003). Sorting nexin 9 participates in clathrin-mediated endocytosis through interactions with the core components. J. Biol. Chem. *278*, 46772–46781.

Lundmark, R., and Carlsson, S. R. (2004). Regulated membrane recruitment of dynamin-2 mediated by sorting nexin 9. J. Biol. Chem. *279*, 42694–42702.

MaCaulay, S. L., Stoichevska, V., Grusovin, J., Gough, K. H., Castelli, L. A., and Ward, C. W. (2003). Insulin stimulates movement of sorting nexin 9 between cellular compartments: a putative role mediating cell surface receptor expression and insulin action. Biochem. J. *376*, 123–134.

Marks, B., Stowell, M. H., Vallis, Y., Mills, I. G., Gibson, A., Hopkins, C. R., and McMahon, H. T. (2001). GTPase activity of dynamin and resulting conformation change are essential for endocytosis. Nature *410*, 231–235.

McNiven, M. A., Kim, L., Krueger, E. W., Orth, J. D., Cao, H., and Wong, T. W. (2000). Regulated interactions between dynamin and the actin-binding protein cortactin modulate cell shape. J. Cell Biol. *151*, 187–198.

Merrifield, C. J., Feldman, M. E., Wan, L., and Almers, W. (2002). Imaging actin and dynamin recruitment during invagination of single clathrin-coated pits. Nat. Cell Biol. *4*, 691–698.

Miele, A. E., Watson, P. J., Evans, P. R., Traub, L. M., and Owen, D. J. (2004). Two distinct interaction motifs in amphiphysin bind two independent sites on the clathrin terminal domain beta-propeller. Nat. Struct. Mol. Biol. *11*, 242–248.

Mundigl, O., Ochoa, G. C., David, C., Slepnev, V. I., Kabanov, A., and De Camilli, P. (1998). Amphiphysin I antisense oligonucleotides inhibit neurite outgrowth in cultured hippocampal neurons. J. Neurosci. *18*, 93–103.

Nakata, T., Iwamoto, A., Noda, Y., Takemura, R., Yoshikura, H., and Hirokawa, N. (1991). Predominant and developmentally regulated expression of dynamin in neurons. Neuron *7*, 461–469.

Nakata, T., Takemura, R., and Hirokawa, N. (1993). A novel member of the dynamin family of GTP-binding proteins is expressed specifically in the testis. J. Cell Sci. *105*(Pt 1), 1–5.

Owen, D. J., Wigge, P., Vallis, Y., Moore, J. D., Evans, P. R., and McMahon, H. T. (1998). Crystal structure of the amphiphysin-2 SH3 domain and its role in the prevention of dynamin ring formation. EMBO J. *17*, 5273–5285.

Peter, B. J., Kent, H. M., Mills, I. G., Vallis, Y., Butler, P. J., Evans, P. R., and McMahon, H. T. (2004). BAR domains as sensors of membrane curvature: the amphiphysin BAR structure. Science *303*, 495–499.

Roos, J., and Kelly, R. B. (1998). Dap160, a neural-specific Eps15 homology and multiple SH3 domain-containing protein that interacts with *Drosophila* dynamin. J. Biol. Chem. *273*, 19108–19119.

Rothman, J. H., Raymond, C. K., Gilbert, T., O'Hara, P. J., and Stevens, T. H. (1990). A putative GTP binding protein homologous to interferon-inducible Mx proteins performs an essential function in yeast protein sorting. Cell *61*, 1063–1074.

Schafer, D. A. (2004). Regulating actin dynamics at membranes: a focus on dynamin. Traffic *5*, 463–469.

Schafer, D. A., Weed, S. A., Binns, D., Karginov, A. V., Parsons, J. T., and Cooper, J. A. (2002). Dynamin2 and cortactin regulate actin assembly and filament organization. Curr. Biol. *12*, 1852–1857.

Schmidt, A., Wolde, M., Thiele, C., Fest, W., Kratzin, H., Podtelejnikov, A. V., Witke, W., Huttner, W. B., and Soling, H. D. (1999). Endophilin I mediates synaptic vesicle formation by transfer of arachidonate to lysophosphatidic acid. Nature *401*, 133–141.

Schmitz, U., Thommes, K., Beier, I., Dusing, R., and Vetter, H. (2004). Identification of Nck interacting proteins in vascular smooth muscle cells. Clin. Exp. Hypertens. *26*, 267–275.

Sever, S., Damke, H., and Schmid, S. L. (2000a). Dynamin:GTP controls the formation of constricted coated pits, the rate limiting step in clathrin-mediated endocytosis. J. Cell Biol. *150*, 1137–1148.

Sever, S., Damke, H., and Schmid, S. L. (2000b). Garrotes, springs, ratchets, and whips: putting dynamin models to the test. Traffic *1*, 385–392.

Sever, S., Muhlberg, A. B., and Schmid, S. L. (1999). Impairment of dynamin's GAP domain stimulates receptor-mediated endocytosis. Nature *398*, 481–486.

Shpetner, H. S., and Vallee, R. B. (1989). Identification of dynamin, a novel mechanochemical enzyme that mediates interactions between microtubules. Cell *59*, 421–432.

Song, B. D., and Schmid, S. L. (2003). A molecular motor or a regulator? Dynamin's in a class of its own. Biochemistry *42*, 1369–1376.

Song, B. D., Yarar, D., and Schmid, S. L. (2004). An assembly-incompetent mutant establishes a requirement for dynamin self-assembly in clathrin-mediated endocytosis in vivo. Mol. Biol. Cell *15*, 2243–2252.

Sontag, J. M., Fykse, E. M., Ushkaryov, Y., Liu, J. P., Robinson, P. J., and Sudhof, T. C. (1994). Differential expression and regulation of multiple dynamins. J. Biol. Chem. *269*, 4547–4554.

Stowell, M. H., Marks, B., Wigge, P., and McMahon, H. T. (1999). Nucleotide-dependent conformational changes in dynamin: evidence for a mechanochemical molecular spring. Nat. Cell Biol. *1*, 27–32.

Takei, K., Slepnev, V. I., Haucke, V., and De Camilli, P. (1999). Functional partnership between amphiphysin and dynamin in clathrin-mediated endocytosis. Nat. Cell Biol. *1*, 33–39.

Thompson, H. M., Cao, H., Chen, J., Euteneuer, U., and McNiven, M. A. (2004). Dynamin 2 binds gamma-tubulin and participates in centrosome cohesion. Nat. Cell Biol. *6*, 335–342.

van der Bliek, A. M., Redelmeier, T. E., Damke, H., Tisdale, E. J., Meyerowitz, E. M., and Schmid, S. L. (1993). Mutations in human dynamin block an intermediate stage in coated vesicle formation. J. Cell Biol. *122*, 553–563.

Warnock, D. E., Baba, T., and Schmid, S. L. (1997). Ubiquitously expressed dynamin-II has a higher intrinsic GTPase activity and a greater propensity for self-assembly than neuronal dynamin-I. Mol. Biol. Cell *8*, 2553–2562.

Warnock, D. E., Terlecky, L. J., and Schmid, S. L. (1995). Dynamin GTPase is stimulated by crosslinking through the C-terminal proline-rich domain. EMBO J. *14*, 1322–1328.

Wigge, P., Kohler, K., Vallis, Y., Doyle, C. A., Owen, D., Hunt, S. P., and McMahon, H. T. (1997). Amphiphysin heterodimers: potential role in clathrin-mediated endocytosis. Mol. Biol. Cell *8*, 2003–2015.

Wigge, P., and McMahon, H. T. (1998). The amphiphysin family of proteins and their role in endocytosis at the synapse. Trends Neurosci. *21*, 339–344.

Wilsbach, K., and Payne, G. S. (1993). Vps1p, a member of the dynamin GTPase family, is necessary for Golgi membrane protein retention in *Saccharomyces cerevisiae*. EMBO J. *12*, 3049–3059.

Worby, C. A., and Dixon, J. E. (2002). Sorting out the cellular functions of sorting nexins. Nat. Rev. Mol. Cell. Biol. *3*, 919–931.

Worby, C. A., Simonson-Leff, N., Clemens, J. C., Kruger, R. P., Muda, M., and Dixon, J. E. (2001). The sorting nexin, DSH3PX1, connects the axonal guidance receptor, Dscam, to the actin cytoskeleton. J. Biol. Chem. *276*, 41782–41789.

Yarar, D., Waterman-Storer, C. M., and Schmid, S. L. (2005). A dynamic actin cytoskeleton functions at multiple stages of clathrin-mediated endocytosis. Mol. Biol. Cell *16*, 964–975.

Yoshida, Y. *et al.* (2004). The stimulatory action of amphiphysin on dynamin function is dependent on lipid bilayer curvature. EMBO J *23*, 3483–3491.

Zhang, B., and Zelhof, A. C. (2002). Amphiphysins: raising the BAR for synaptic vesicle recycling and membrane dynamics. Bin-Amphiphysin-Rvsp. Traffic *3*, 452–460.